Journal Home Page: https://sjes.univsul.edu.iq/

Calculating Drought Hazard and Drought Risk Indices for Mandawa Basin in Kurdistan Region, Iraq Using Spatial Analysis Tools

Zhian Abdulrahman Ahmed[1,a,*]
Jehan Mohammed Fattah[2,a]

[a] Department of Water Resources Engineering, College of Engineering, Salahaddin University-Erbil, Kurdistan Region, Iraq

Article Information

Article History:
Received: February 11th 2025
Accepted : November 29, 2025
Available online: December, 2025

Keywords:
Hydrological Drought, DHI, DRI, SPI, SPEI

About the Authors:
Corresponding author:
Zhian Abdulrahman Ahmed
E-mail: zhiyan.ahmed@su.edu.krd
Researcher Involved:
Assist. Proof. Dr. Jehan Mohammed Fattah
E-mail:
jehanmohammed.sheikhsuleimany@su.edu.krd

DOI https://doi.org/10.17656/sjes.102006

Abstract

Drought is a global environmental disaster with wide-ranging impacts. This work uses different drought indicators to assess the areas prone to hydrological drought of the Mandawa basin with in Iraqi Kurdistan Region. Other trends were found in the drought hazard study utilizing meteorological drought indices. According to the Standardized Precipitation Index (SPI) -based Drought Hazard Index (DHI), the mild, moderate, severe, and extreme drought hazard categories accounted for 16.93%, 39.03%, 25.54%, and 18.45% of the total watershed area, respectively. While the SPEI-DHI map showed that these categories account for 33.63%, 20.52%, 37.39%, and 8.45%, respectively. The Drought Risk Index (DRI) map results for both SPI and SPEI revealed that the majority of the study area falls into the low and very low drought risk categories, accounting for 70% and 50% for SPI-DRI and SPEI-DRI, respectively. The SPEI-DRI determined that 23.17% of the study area is in the high drought risk category, which is twice the area determined by the SPI-DRI. However, this index was more sensitive in determining the very high drought risk category, which accounts for 14%.

1. Introduction

Globally, drought is a significant natural hazard that affects both environment and society in many different ways [1]. Since water is essential for many human activities, hydrological drought has a wide range of impacts on our lives, such as increased water demands, water supply contamination, and salinization [2]. In Iraq, most studies have focused on agricultural or meteorological droughts, while very few studies are available for hydrological droughts, as will be explained below Fadhil [3], Gaznayee and Quraishi [4], and Gaznayee et al. [5] evaluated agricultural drought in the Kurdistan Region of Iraq using the Normalized Differential Water Index (NDWI) and the Normalized Difference Vegetation Index (NDVI) between the years (2007 to 2008; 1998 to 2012; 1998 to 2017), respectively. Their results indicated that 2008 was an extremely dry year, and the frequency and severity of droughts had increased, particularly between 2000 and 2008. In Kurdistan region of Iraq, Al-Hedny and Muhaimeed [6] and Yenigun and Ibrahim [7] used the SPI of 1, 3, 6, 9, and 12 months and NDVI during years (1979 to 2013; 1980 to 2010), respectively, to investigate agricultural drought. According to their results, 2008 was the driest year on record, and the NDVI had an evident impact on SPI-6. Hasan and Saeed [8] investigated hydrological drought for three rivers in the north of Iraq for the years 1965-2011 by using mean monthly stream discharges to determine the stream-flow drought index (SDI), indicating that the hydrological drought was increasing. Research by Jameel et al. [9] was performed using SPEI for one- and three-month periods, together with the SPI, to illustrate the trend of the drought conditions in northern Iraq from 1980 to 2020. The study discovered deficiencies in the region's groundwater, surface water, and soil moisture levels after 1997, in addition to the substantial

consequences of the drought that had lasted for the previous 20 years. Jameel et al. [9], Hamed et al. [10] and Jasim and Awchi [11] conducted a study on meteorological drought in Iraq between 2000 and 2011, 1970 and 2013, and 1975 and 2014, respectively. The results revealed that the driest year was 2008, while 2001 and 2003 were the wetter years. In addition, the two years with the worst droughts were 1997 to 2001 and 2007 to 2010. Furthermore, the results indicate that in the near future, the frequency of droughts dropped between 0 and 40%, while in the far future, the frequency of moderate and severe droughts increased by up to 45%.

This work investigates the hydrological drought indices, using RS, GIS, and different meteorological indicators based on precipitation data for the basin under research. The significance of this research lies in its pioneering attempts to assess the region's susceptibility to drought, which will improve the preparation and management of drought-related difficulties across multiple sectors.

2. Methods and Materials

2.1. The research area

The Mandawa basin covers an area of approximately 3542.5 km² of area and is located in the Kurdistan Region of northeastern Iraq, and the continental climate of the research region is dry and semi-arid [12]. See Figure 1.

2.2. Data Collection

Meteorological data pertaining to historical records of average monthly rainfall (P) and temperature (T) datasets were collected for the watershed for a period of 20 years, from 2002-2021, for six stations distributed in and around the study area; as shown in Figure 1. This multiyear period was chosen as a baseline due to the limited availability of temperature data. The data were collected from Meteorological Department of the Ministry of Agriculture and Water Resources, Kurdistan Regional Government (KRG), Iraq and the information of precipitation and temperature at the six meteorological stations during the selected period are shown in the study published by Zhian and Sulemany [12].

2.3. Metrological drought indices

The SPI is a meteorological drought index that measures the deviation from the long-term mean by calculating the precipitation deficit or surplus [13]. In this investigation monthly rainfall data collected at six rainfall stations between 2002 and 2021 were used to calculate SPI values, and were fitted to a gamma distribution created by Guttman [14] as shown in Eq.1, and then standardized to a normal distribution with a mean of zero and a variance of one.

$$g(x,\alpha,\beta) = \frac{1}{\beta^{\alpha} * \Gamma(\alpha)}\, x^{\alpha-1}\, e^{-\frac{x}{\beta}} \qquad (1)$$

Where x is a precipitation measurement, α > 0 and β > 0 stand for shape and scale parameters, respectively, and Γ (α) is the Gamma function.

Various probability distributions, such as log-logistic, gamma, and Pearson Type III, are commonly used for SPI calculations [6, 15, 16]. Drought classifications based on SPI developed by McKee et al. [13] are shown in Table 1.

The SPEI is a multi-scalar drought index that utilizes the monthly difference (D) between precipitation (P) and potential evapotranspiration (PET) depending on the SPI created by Vicente-Serrano et al. [17]. This D, which is calculated as follows, is the simple climatic balance for a specific month (i).

$$D_i = P_i - PET_i \qquad (2)$$

Various empirical equations exist to calculate potential evapotranspiration (PET) from climatic data. Due to limited data, the empirical formula by Thornthwaite [18], which considers latitude and temperature, was used to estimate monthly PET in this research. After that, the climatic water balance (D) was calculated and fitted to a probability distribution function (PDF) using three parameters. Selecting the most suitable distribution for D is challenging, as different studies recommend different distributions [19-21]. When compared to other distributions, the three-parameter log-logistic distribution was determined to fit the climatic water balance series the best by [22] in their original study. Table (2) shows moisture categories according to SPEI values developed by [22]. In Iraq, [23-25] used the log-logistic distribution for SPEI calculation. Eventually, the log-logistic probability density function was employed to fit the series, as shown below:

$$f(x) = \frac{\beta}{\alpha}\left(\frac{x-\gamma}{\alpha}\right)^{\beta-1}\left[1+\left(\frac{x-\gamma}{\alpha}\right)^{\beta}\right]^{-2} \qquad (3)$$

2.4. Drought Identification

Drought indices provide a time series of data values implying an excess or deficit of water in contrast to its overall average availability. To explore the characteristics of the drought of the six selected stations in the 20-year statistical period, SPEI and SPI drought indices were computed at a time scale of 12 months. This time scale may provide an annual estimate of water conditions, such as reservoir levels, stream flows, and sometimes even groundwater levels. The SPI scale is used to characterize droughts for both SPI and SPEI. This scale is used because both indices are calculated using the same principles. This study focuses on mild to extreme droughts, and the SPI/SPEI index scale is shown in Table (1). It should be mentioned that a drought starts when the value of the index falls below a certain threshold and continues until it exceeds the selected threshold value. A zero threshold was utilized in this study to identify drought events, and the characteristics of each drought event, such as severity, duration, and peak, were extracted.

There are several methods for determining the drought threshold, but choosing zero is one of the most practical and straightforward method. Following the identification of drought events, the run theory method was used to determine the severity, duration, and peak of each drought event, which is one of the most useful methods for extracting drought characteristics. The copulas method is another similar method. However, the run theory method was used in this study because of its simplicity.

2.5. Correlation between SPI and SPEI

The relationship between SPI and SPEI was evaluated using the **Pearson correlation coefficient (R)** at the 99% confidence level. It was calculated as:

$$R_{xy} = \frac{\sum_{i=1}^{n}(x_i-\bar{x})(y_i-\bar{y})}{\sqrt{\sum_{i=1}^{n}(x_i-\bar{x})^2(y_i-\bar{y})^2}} \quad (4)$$

Where n is the number of observations, and x and y represent SPI and SPEI values, respectively. R ranges from –1 to +1, with $|R| \geq 0.5$ indicating a strong correlation between the two indices.

2.6. Drought Hazard Index (DHI)

Drought Hazard presents a complete description of the frequency and intensity of drought events [25]. Drought events and their intensities are computed using SPEI and SPI because both indices are accepted and suitable tools for monitoring drought events and can be calculated for different time scales and thus can be linked to various types of drought: meteorological drought (1 month), soil moisture drought (3 months), and hydrological drought (12 months). The long-term SPI and SPEI (12 months) have been used to assess and characterize the watershed's hydrological drought. Because different drought intensities do not contribute equally to quantifying and mapping the drought hazard, weight was assigned to each class of drought as shown in Tables 1 and 2. The Jenks natural break method is a data classification method that determines the best way to arrange values into different classes [26]. The probability of occurrence of each drought class using the Jenks natural break method is calculated by dividing the frequency of occurrence for each class by the number of possible states in each station [27]. This is accomplished by attempting to minimize the average deviation of each class from the class while maximizing each class's deviation from the means of the other groups [28]. Table (3) illustrates the weights and ratings assigned to each case. Finally, the DHI for each index is computed by combining weights and ratings as shown below:

$$DHI = MiD_w * MiD_r + MoD_w * MoD_r + SeD_w * SeD_r + ExD_w * ExD_r \quad (5)$$

Where Mi, Mo, Se, and Ex stand for mild, moderate, severe, and extreme, respectively. While Dw and Dr stand for weights and ratings of draughts, respectively. As a final step, the spatial extent of drought hazard for each index (SPI and SPEI) is derived by interpolating the DHI values of each station using the inverse distance weighted (IDW) interpolation method in the geostatistical analysis tool in ArcGIS software.

2.7. Drought Risk Index (DRI)

Drought risk is computed as the product of the Drought Vulnerability Index (DVI) and the DHI [29]. For the Mandawa basin , Zhian and sulemany [12] adopted seven causative factors that has an effect on the drought vulnerability: slope, land use and land cover, soil texture, temperature, precipitation, distance to rivers, and elevation to estimate DVI.

$$DVI = \sum_{i=1}^{n} w_i * x_i \quad (6)$$

Where, n is number of factors, w_I is weight of the criteria and x_I is the priority rating of the factor. And then eq. 7 is used to find the areas under drought risk.

$$DRI = DVI * DHI \quad (7)$$

Because of the product relationship, if there is no vulnerability or hazard, the drought risk for that location is zero. Higher DVI or DHI values, on the other hand, indicate an increased risk of the drought event. Therefore, the drought risk of the area is determined by the DHI and DVI values. The DRI data were then categorized into different classes using the natural break approach in ArcGIS software.

3. Results and Discussion

3.1. Drought Identification

The 12-month SPI and SPEI indices for six stations in the Mandawa watershed (2002–2021) were computed using the SPEI package in R to evaluate temporal drought variability. Figures 2 and 3 show the time series of SPI and SPEI at all stations, illustrating the temporal patterns of drought events. Both indices captured similar patterns of drought events, although SPEI was generally more sensitive, detecting extreme events missed by SPI. For instance, at Pirmam station, SPEI identified nine extreme drought events (3.37% of total events), while SPI detected none (Table 4, Figures 4–5). Mild droughts were the most frequent across all stations, followed by moderate, severe, and extreme events. Major drought years included 2007–2009, 2011–2012, 2014, 2017–2018, and 2021, consistent with Gaznayee et al. (2022a). SPI and SPEI sometimes differed in event severity; for example, SPEI indicated 2014 as wet for most stations, whereas SPI recorded mild drought, and after 2017, SPEI became more responsive to high-severity droughts, with 2021 showing the highest severity across most stations. This highlights the increasing influence of temperature on drought in recent years. The drought

characteristics extracted using SPI and SPEI at 12-month scales (Tables 5–6) revealed long-duration events at Khabat station (SPI: 69 months, SPEI: 49 months). Peak drought severity was similar across indices, generally below –2, with the most intense peaks observed in Akre (SPI: –2.4, Feb 2009) and Soran (SPEI: –2.41, Apr 2008). Overall, SPEI proved more sensitive in detecting both duration and extreme droughts, reflecting the combined effects of precipitation deficits and increased evaporative demand.

3.2. Correlation between SPI and SPEI

The correlation between SPI and SPEI at a 12 month time scale for different stations in the Mandawa watershed is investigated using the Pearson Correlation Coefficient (R). The test results revealed a strong and significant relationship between SPI and SPEI at $P<0.01$, with values ranging from 0.71-0.97. Northern stations had a stronger correlation between SPI and SPEI compared to southern stations. This pattern is most likely due to southern stations having higher average annual temperatures than northern stations. This could imply that air temperature is a significant factor at the watershed. Nonetheless, the high correlation between SPI and SPEI at stations such as Soran demonstrates that both indices are dependable and that SPI can represent drought circumstances on its own. The correlation between SPI and SPEI at the stations is illustrated in Figure 6.

3.3. Drought hazard

After determining the probability of drought occurrence for each drought category for both indices as shown in Table 4, the DHI maps for each drought index (SPI and SPEI) were calculated. Each index's geographical extent (hazard map) was divided into four groups: mild, moderate, severe, and extreme drought hazards. Table (7) displays the DHI classes for both indices. (Figures 7 and 8) depict the area's SPI and SPEI-classified drought hazard map. Based on SPI-DHI results, the majority of the study area (nearly 39.03%) experiences moderate drought hazard, primarily in the central and northern-middle parts of the watershed. Southern and northeastern regions are extremely and severely drought-prone. SPEI-DHI findings reveal that a significant portion of the study area (about 38% of the total watershed area) is categorized as a severe drought hazard, mainly in the western parts from north to south. Regions dominated by SPI-based droughts with extreme DHI are larger than those dominated by lower DHI of SPEI-based droughts in the severe drought category.

3.4. Drought risk

(Figures 9 and 10) display the spatial pattern of DRI for SPI and SPEI, while Table (8) shows the percentage of area in each drought risk category. The SPI-based drought risk map shows that most of the study area (about 70%) is located in the upper-middle section of the watershed and falls into the combined extremely low and low drought risk categories. On the other hand, these categories represent 50% of the SPEI-based drought risk map and encompass the northeastern part of the research area. Furthermore, the SPEI-DRI emphasizes that the 820.88 km² northwest to southwest region is classified as having a high risk of drought. This area is twice the size indicated by the DRI of SPI, mainly due to the higher probability of severe drought occurrences indicated by the SPEI-based DHI. Both drought risk indices exhibit similar patterns for the very high drought risk class, primarily covering the southern parts of the watershed. However, the DRI of SPI tends to indicate more areas under this category compared to the DRI of SPEI, mainly due to the sensitivity of SPI-based DHI in identifying extreme drought hazard classes.

4. Conclusions

This study provides a summary of the following points.

•The SPI-DHI map demonstrates that the research area's northeastern and southern regions are the most likely to experience severe and extreme drought, which is largely because of the high probability of severe drought occurrences in Shaqlawa, Khabat, and Ainkawa stations. While the northwestern and middle parts of the watershed are the least likely.

•The degree of SPEI-DHI is lowest in the watershed's north-eastern portion and highest in the watershed's north-western and southern portions. DHI of SPI dominated more regions with extreme drought categories than DHI of SPEI, which was more sensitive in predicting severe droughts. In general, these two categories are more likely to occur in areas south of the watershed.

•The SPI and SPEI drought risk maps reveal that the majority of the upper middle parts of the study area are not at risk of drought, except the northwestern parts, as indicated by the SPEI-DRI, whereas the lower middle parts are severely or extremely at risk of drought.

Declarations: All authors have read, understood, and complied as applicable with the statement on "Ethical responsibilities of Authors" as found in the Instructions for Authors.

Data availability: During the current investigation, no datasets were created or examined.

Acknowledgement: The authors would like to express their gratitude to Salahaddin University-Erbil-Iraq for providing them with the required resources to complete this article.

Competing interests: The authors declare no competing interests

Funding: There was no funding for this study

References

[1] A. F. Van Loon and G. Laaha, "Hydrological drought severity explained by climate and

catchment characteristics," *Journal of hydrology,* vol. 526, pp. 3-14, 2015.

[2] M. Mirakbari and M. Entezari, "Joint modeling of drought and dust hazards using copula-based model over Iran from 1988 to 2018," *Stochastic Environmental Research and Risk Assessment,* vol. 37, pp. 4029-4050, 2023.

[3] A. M. Fadhil, "Drought mapping using Geoinformation technology for some sites in the Iraqi Kurdistan region," *International Journal of Digital Earth,* vol. 4, pp. 239-257, 2011.

[4] H. Gaznayee and A. Al-Quraishi, "Identifying drought status in Duhok Governorate (Iraqi Kurdistan Region) from 1998 through 2012 using landsat time series dataset," *Journal of Applied Science and Technology Trends,* vol. 1, pp. 17-23, 2020.

[5] H. A. A. Gaznayee, A. M. F. Al-Quraishi, K. Mahdi, J. P. Messina, S. H. Zaki, H. A. S. Razvanchy*, et al.*, "Drought severity and frequency analysis aided by spectral and meteorological indices in the kurdistan region of Iraq," *Water,* vol. 14, p. 3024, 2022.

[6] S. M. Al-Hedny and A. S. Muhaimeed, "Drought monitoring for Northern Part of Iraq using temporal NDVI and rainfall indices," in *Environmental remote sensing and GIS in Iraq*, ed: Springer, 2019, pp. 301-331.

[7] K. Yenigun and W. A. Ibrahim, "Investigation of drought in the northern Iraq region," *Meteorological Applications,* vol. 26, pp. 490-499, 2019.

[8] I. F. Hasan and Y. N. Saeed, "Trend analysis of hydrological drought for selected rivers in Iraq," *Tikrit Journal of Engineering Sciences,* vol. 27, pp. 51-57, 2020.

[9] M. Jameel, S. Hameed, K. Shemal, N. Al-Ansari, and S. A. Abed, "Spatial and temporal assessment of drought in the northern prone of Iraq using standardized precipitation index," *Engineering,* vol. 15, pp. 691-708, 2023.

[10] M. M. Hamed, S. S. Sammen, M. S. Nashwan, and S. Shahid, "Spatiotemporal changes in droughts in Iraq for shared socioeconomic pathways," 2022.

[11] A. I. Jasim and T. A. Awchi, "Regional meteorological drought assessment in Iraq," *Arabian Journal of Geosciences,* vol. 13, p. 284, 2020.

[12] Z. A. Ahmed and J. M. Fattah Sheikh Suleimany, "Drought vulnerability modeling over Mandawa watershed, northern Iraq, using GIS-AHP techniques," *Polytechnic Journal,* vol. 12, p. 15, 2023.

[13] T. B. McKee, N. J. Doesken, and J. Kleist, "The relationship of drought frequency and duration to time scales," in *Proceedings of the 8th Conference on Applied Climatology*, 1993, pp. 179-183.

[14] N. B. Guttman, "Accepting the standardized precipitation index: a calculation algorithm 1," JAWRA *Journal of the American Water Resources Association,* vol. 35, pp. 311-322, 1999.

[15] A. M. Al-Quraishi, H. A. Gaznayee, and M. Crespi, "Drought trend analysis in a semi-arid area of Iraq based on normalized difference vegetation index, normalized difference water index and standardized precipitation index," *Journal of Arid Land,* vol. 13, pp. 413-430, 2021.

[16] S. Patil, "Analysis of Spatial Performance of Meteorological Drought Indices," 2013.

[17] S. M. Vicente-Serrano, S. Beguería, and J. I. López-Moreno, "A multiscalar drought index sensitive to global warming: the standardized precipitation evapotranspiration index," *Journal of climate,* vol. 23, pp. 1696-1718, 2010.

[18] C. W. Thornthwaite, "An approach toward a rational classification of climate," *Geographical review,* vol. 38, pp. 55-94, 1948.

[19] M. Hameed, A. Ahmadalipour, and H. Moradkhani, "Apprehensive drought characteristics over Iraq: results of a multidecadal spatiotemporal assessment," *Geosciences,* vol. 8, p. 58, 2018.

[20] S.Poornima and M. Pushpalatha, "RETRACTED ARTICLE: Drought prediction based on SPI and SPEI with varying timescales using LSTM recurrent neural network," *Soft Computing,* vol. 23, pp. 8399-8412, 2019.

[21] Q. Wang, J. Zeng, J. Qi, X. Zhang, Y. Zeng, W. Shui*, et al.*, "A multi-scale daily SPEI dataset for drought characterization at observation stations over mainland China from 1961 to

2018," *Earth System Science Data,* vol. 13, pp. 331-341, 2021.
[22]W.-G. LI, X. YI, M.-T. HOU, H.-L. CHEN, and Z.-L. CHEN, "Standardized precipitation evapotranspiration index showsdrought trends in China," *Chinese Journal of Eco-Agriculture,* vol. 20, pp. 643-649, 2012.
[23]R. Albarakat, M.-H. Le, and V. Lakshmi, "Assessment of drought conditions over Iraqi transboundary rivers using FLDAS and satellite datasets," *Journal of Hydrology: Regional Studies,* vol. 41, p. 101075, 2022.
[24]O. M. Mahmood Agha and Y. H. Al-Aqeeli, "Analysis of the standardized precipitation evapotranspiration index over Iraq and its relationship with the Arctic Oscillation Index," *Hydrological Sciences Journal,* vol. 66, pp. 278-288, 2021.
[25]Q. Zhang and J. Zhang, "Drought hazard assessment in typical corn cultivated areas of China at present and potential climate change," *Natural Hazards,* vol. 81, pp. 1323-1331, 2016.
[26]H. Tang, T. Wen, P. Shi, S. Qu, L. Zhao, and Q. Li, "Analysis of Characteristics of Hydrological and Meteorological Drought Evolution in Southwest China," *Water,* vol. 13, p. 1846, 2021.
[27]D. Rajsekhar, V. P. Singh, and A. K. Mishra, "Integrated drought causality, hazard, and vulnerability assessment for future socioeconomic scenarios: An information theory perspective," *Journal of Geophysical Research: Atmospheres,* vol. 120, pp. 6346-6378, 2015.
[28]J. Chen, S. Yang, H. Li, B. Zhang, and J. Lv, "Research on geographical environment unit division based on the method of natural breaks (Jenks)," *The International Archives of the Photogrammetry, Remote Sensing and Spatial Information Sciences,* vol. 40, pp. 47-50, 2013.
[29]A. Ahmadalipour, H. Moradkhani, and M. C. Demirel, "A comparative assessment of projected meteorological and hydrological droughts: elucidating the role of temperature," *Journal of Hydrology,* vol. 553, pp. 785-797, 2017.

حساب مؤشرات مخاطر الجفاف ومؤشرات خطر الجفاف لحوض ماندوا في إقليم كردستان العراق باستخدام أدوات التحليل المكاني

المستخلص:

الجفاف هو كارثة بيئية عالمية ذات آثار واسعة النطاق. يستخدم هذا العمل مؤشرات جفاف مختلفة لتقييم المناطق المعرضة للجفاف الهيدرولوجي في حوض ماندوا بمنطقة كردستان العراقية. كما تم اكتشاف اتجاهات أخرى في دراسة مخاطر الجفاف باستخدام مؤشرات الجفاف المناخية. وفقًا لمؤشر الجفاف المستند إلى مؤشر الهطول القياسي – (SPI) مؤشر مخاطر الجفاف(DHI) ، مثلت فئات الجفاف الخفيف، المتوسط، الشديد، والشديد جداً ١٦.٩٣٪، ٣٩.٠٣٪، ٢٥.٥٤٪، و١٨.٤٥٪ من إجمالي مساحة الحوض على التوالي. بينما أظهرت خريطة DHI المستندة إلى SPEI أن هذه الفئات تمثل ٣٣.٦٣٪، ٢٠.٥٢٪، ٣٧.٣٩٪، و٨.٤٥٪ على التوالي. أظهرت نتائج خريطة مؤشر خطر الجفاف (DRI)لكل من SPI و SPEIأن غالبية منطقة الدراسة تقع ضمن فئات منخفضة ومنخفضة جداً لمخاطر الجفاف، حيث تمثل ٧٠٪ و٥٠٪ بالنسبة لـ . SPI–DRI و SPEI–DRIعلى التوالي. كما بيّنت خريطة SPEI–DRI أن ٢٣.١٧٪ من منطقة الدراسة تقع ضمن فئة مخاطر الجفاف العالية، وهي ضعف المساحة التي تم تحديدها بواسطة .SPI–DRI ومع ذلك، أظهر هذا المؤشر حساسية أكبر في تحديد فئة مخاطر الجفاف العالية جداً، والتي تمثل ١٤٪ من المنطقة.

الكلمات المفتاحيه:

لجفاف الهايدرولوجى، SPI ، SPEI ، **DHI** ، **DRI**

Table 1: The drought classifications [13].

Drought category	SPI Values
Mild Drought	0 to - 0.99
Moderate Drought	-1.00 to -1.49
Severe Drought	-1.50 to -1.99
Extreme Drought	≤ -2.00

Table 2: The SPEI Classification [22]

Classification	SPEI
Extremely wet (EW)	2.0 or more
Very wet(VW)	1.5 to 1.99
Moderately wet(MW)	1.0 to 1.49
Normal (N)	-0.99 to 0.99
Moderately dry(MD)	-1.0 to -1.49
Sever dry(SD)	-1.50 to -1.99
Extremely dry(ED)	-2 and less

Table 3: Weights and ratings assigned to each drought category and probability of occurrence at a time scale of 12 months.

Category	Weight	Occurrence probability	Rating
Mild drought	1	low Very low High Very high	1 2 3 4
Moderate drought	2	low Very low High Very high	1 2 3 4
Severe drought	3	low Very low High Very high	1 2 3 4
Extreme drought	4	low Very low High Very high	1 2 3 4

Table 4: Probability of occurrences of different categories of droughts based on both indices for all stations in the Mandawa area.

Type of Drought Hazard	Mild		Moderate		Severe		Extreme	
Index	**SPI**	**SPEI**	**SPI**	**SPEI**	**SPI**	**SPEI**	**SPI**	**SPEI**
Station								
Khabat	27.58	30.42	9.58	10.42	7.08	7.05	0	0
Ainkawa	37.58	30.42	6.67	11.25	6.67	3.33	0	3.33
Pirmam	27.5	27.08	13.33	8.75	3.75	3.75	0	3.75
Shaqlawa	27.92	33.33	10.42	5.42	5.83	8.33	0.83	0.42
Soran	27.92	31.25	10.83	10	2.08	2.08	2.92	3.33
Akre	25	31.25	11.67	7.08	5	5.42	0.83	2.92

Table 5: Drought characteristics based on SPI

Stations	Number of dry periods	Max duration of dry period	Duration	Peak	Date of occurrence
Khabat	5	69	April 2007-Dec 2012	-1.95	Dec 2009
Shaqlawa	8	26	Nov 2007-Dec 2009	-2.17	Jan 2009
Pirmam	6	30	Oct 2007-March 2010	-1.83	Feb 2009
Soran	6	63	Oct 2007- Dec 2012	-2.31	Feb 2009
Akre	10	26	Oct 2007-Nov 2009	-2.42	Feb 2009
Ainkawa	8	28	Oct 2007-Jan 2010	-2.2	Nov 2021

Table 6: Drought characteristics based on SPEI

Stations	Number of dry periods	Max duration of dry period	Duration	Peak	Date of occurrence
Khabat	9	49	Aug 2007-Sep 2011	-1.95	Dec 2021
Shaqlawa	8	28	Oct 2007-Jan 2010	-2.11	Nov 2021
Pirmam	6	29	Aug 2010-Dec 2012	-2.38	Nov 2021
Soran	9	30	Jul 2010-Dec 2012	-2.41	Apr 2008
Akre	10	26	Oct 2007-Nov 2009	-2.38	Aug 2021
Ainkawa	6	39	Sep 2006-Nov 2009	-2.25	Aug 2021

Table 5: Drought Hazard Classification Area.

Type of Drought Hazard	Area (Km^2)		Area (%)	
	SPI	SPEI	SPI	SPEI
Mild drought hazard	601.66	1191.44	16.93	33.63
Moderate drought hazard	1382.71	727	39.03	20.52
Severe drought hazard	904.68	1324.46	25.54	37.39
Extreme drought hazard	653.56	299.37	18.45	8.45

Table 6: Drought Risk Classification Area

Drought risk category	Area (Km^2)		Area (%)	
	SPI	SPEI	SPI	SPEI
Very low drought risk	1118.16	1440.27	31.56	40.66
Low drought risk	1268.75	444.36	35.81	12.54
Moderate drought risk	181.64	497.03	5.13	14.03
High drought risk	467.01	820.88	13.18	23.17
Very high drought risk	507.07	340.09	14.31	9.60

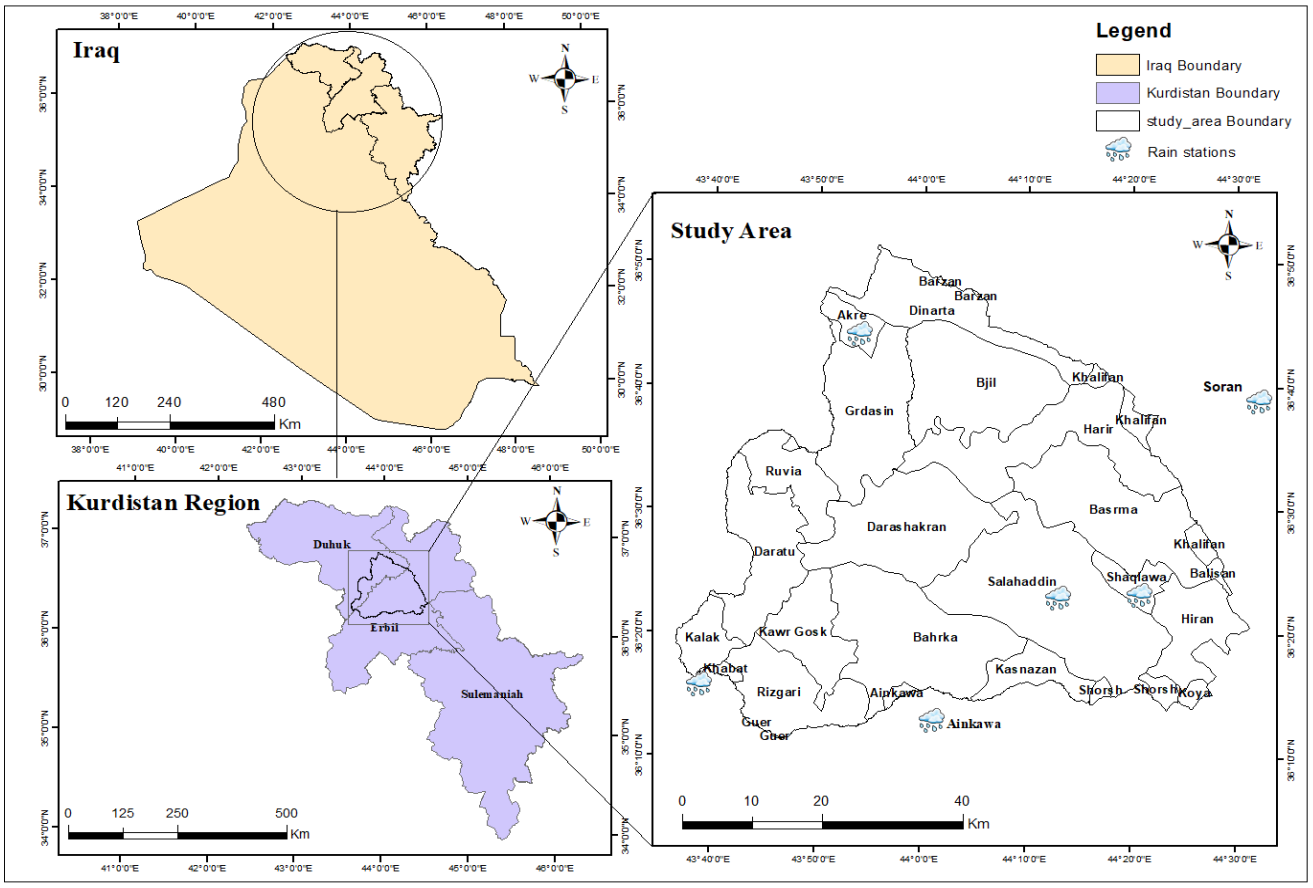

Figure 1. Illustration of the area under research

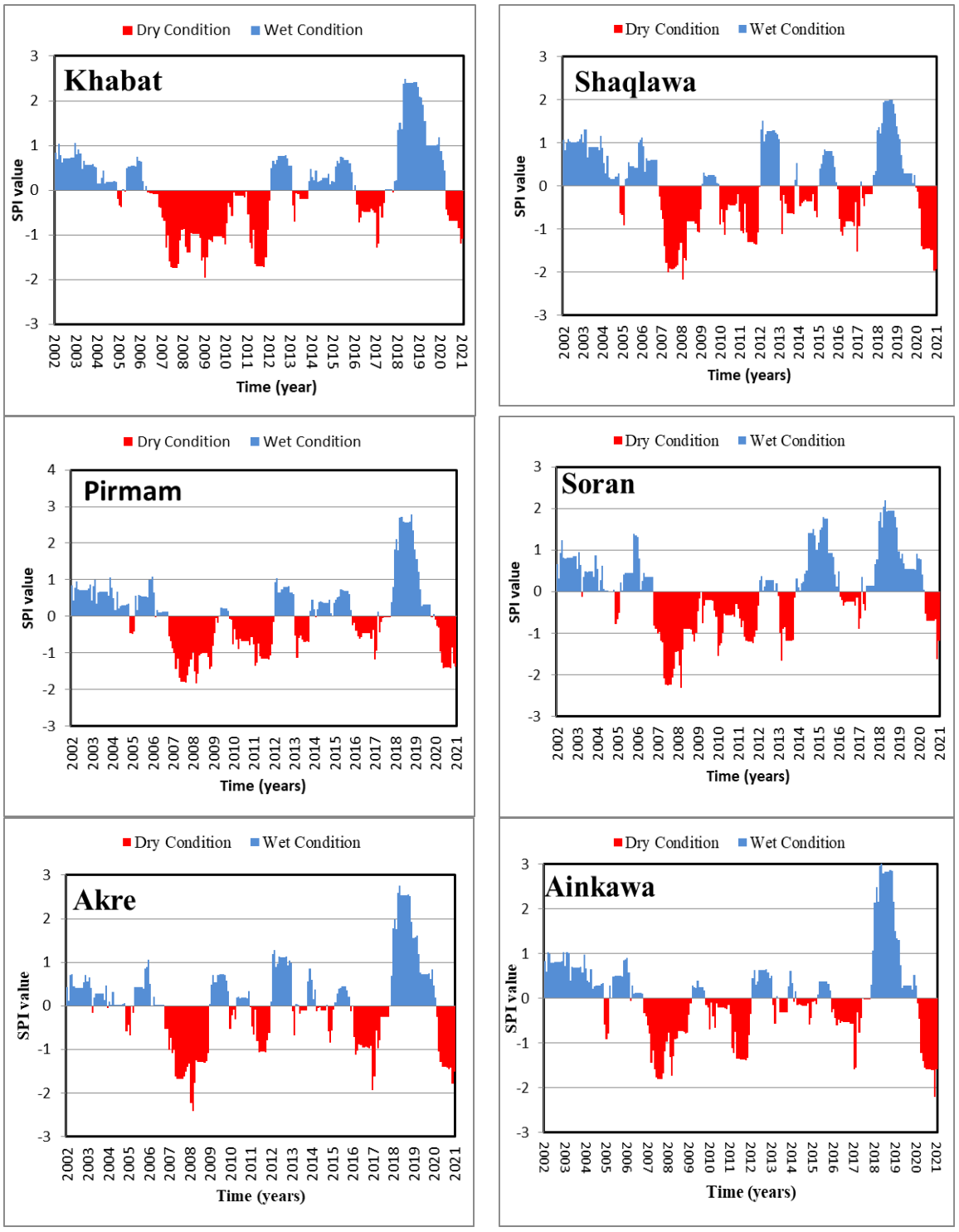

Figure 2: The SPI results at all stations

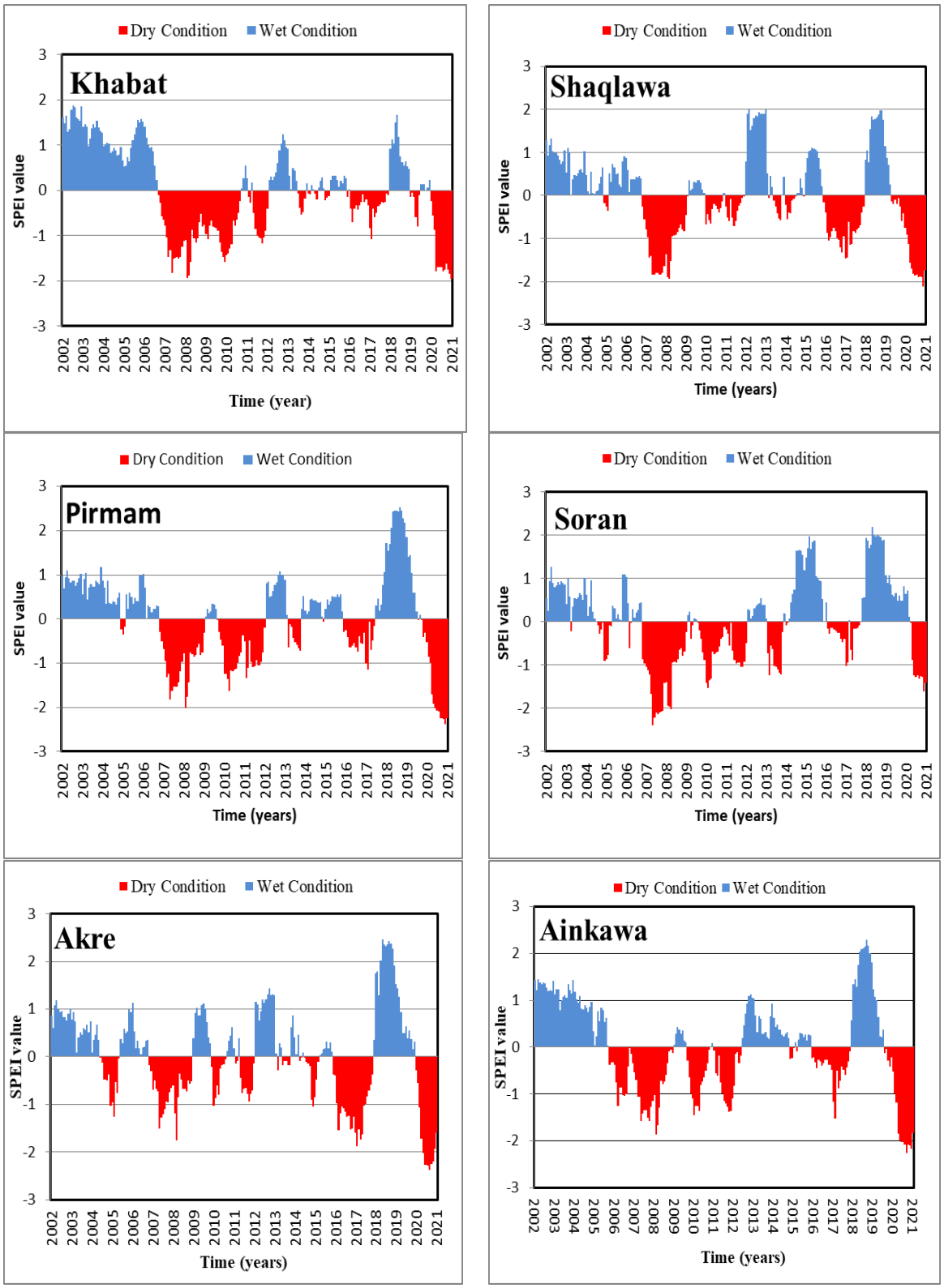

Figure 3: The SPEI results at all stations

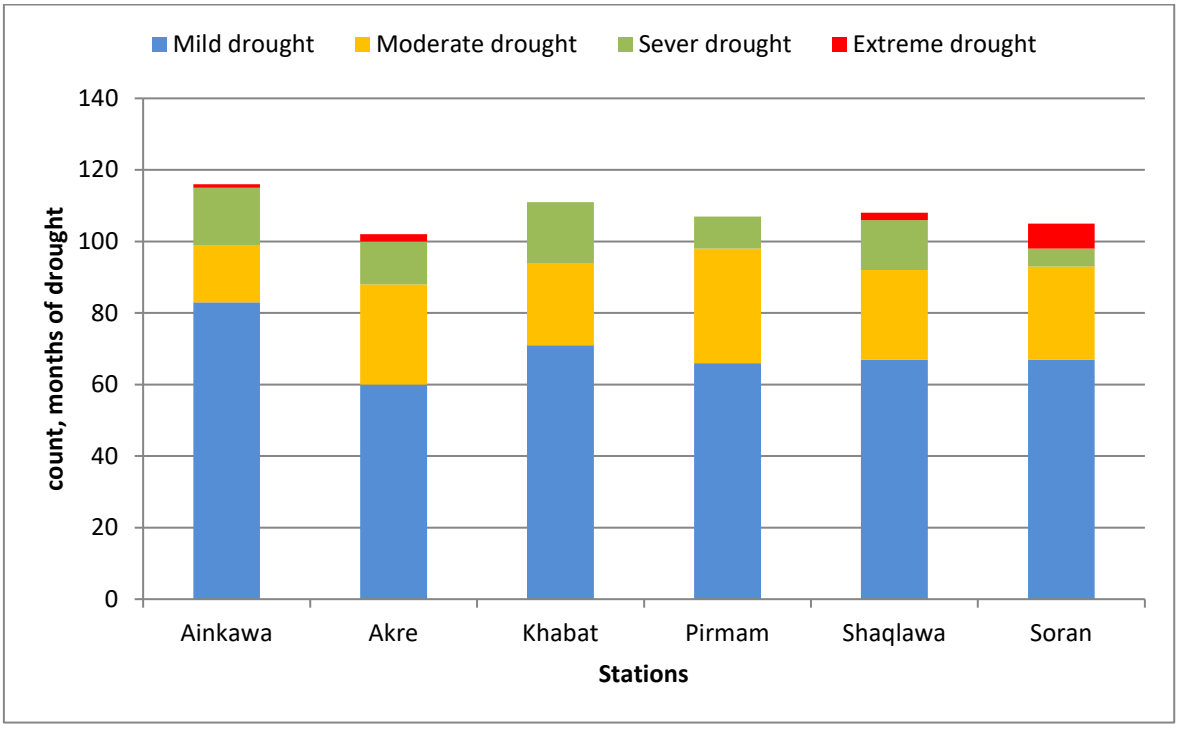

Figure 4: Number of drought events (2002-2021) according to SPI

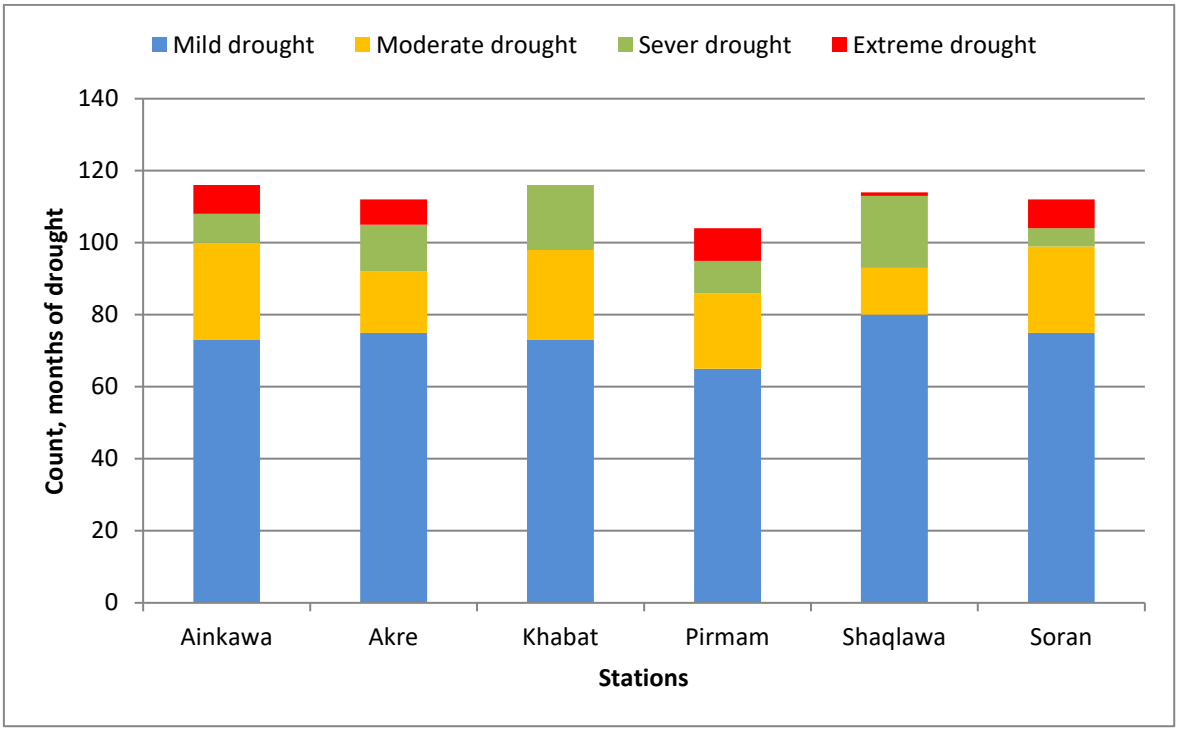

Figure 5: Number of drought events (2002-2021) according to SPEI

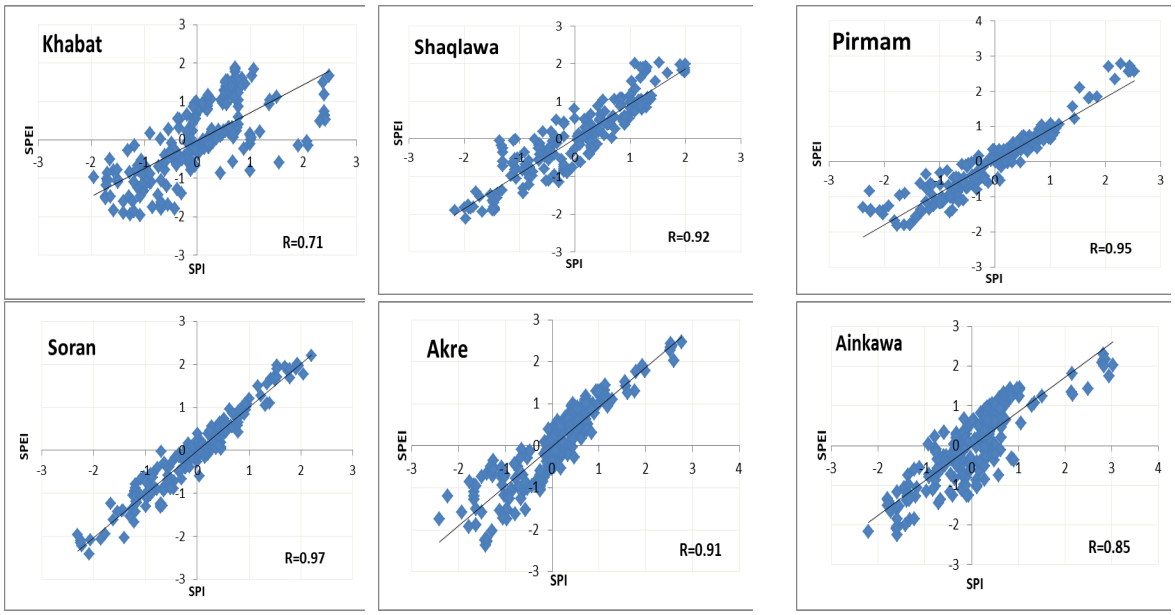

Figure 6: Correlation between SPI and SPEI at selected stations

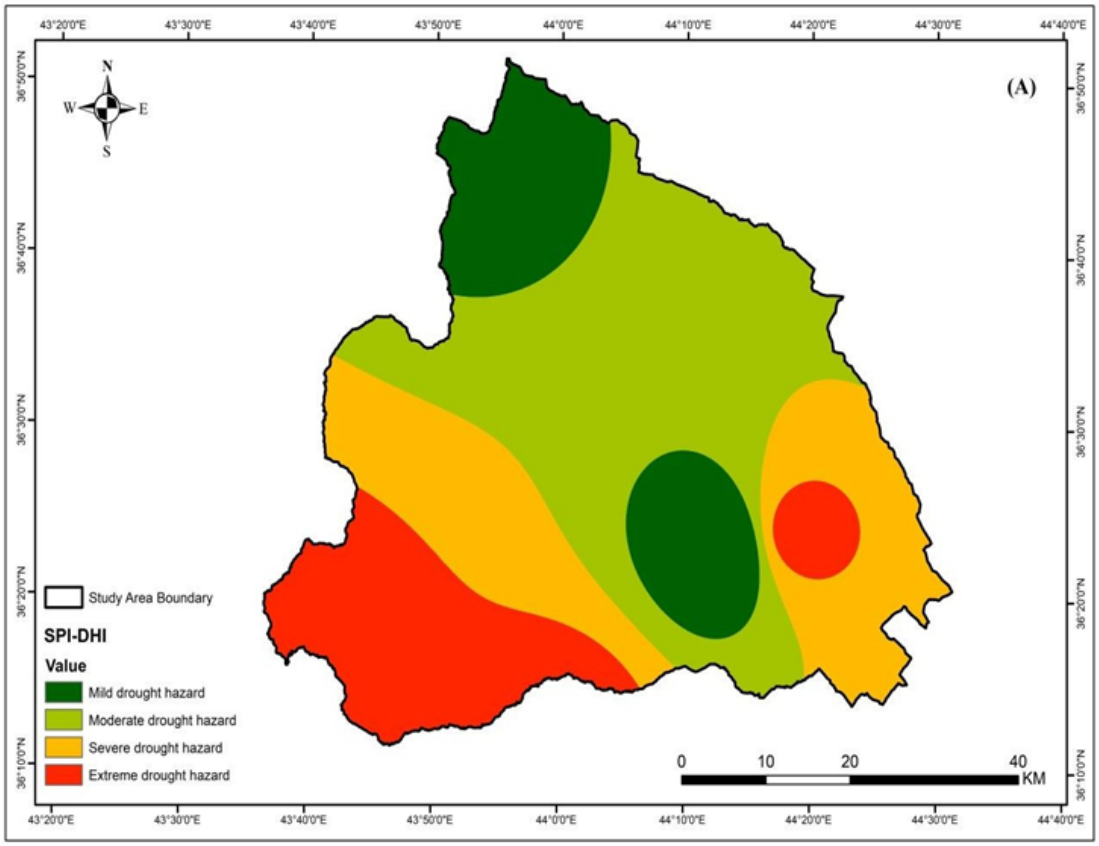

Figure 7: The DHI of the watershed based on SPI.

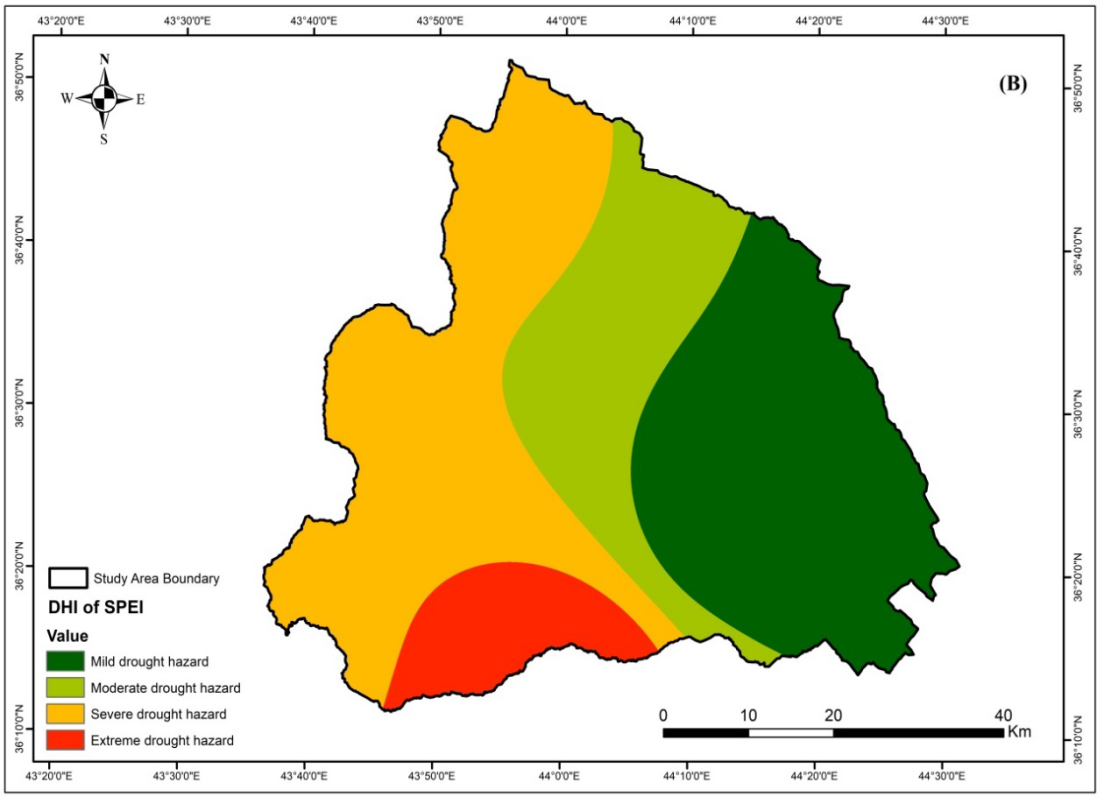

Figure 8: The DHI of the watershed based on SPEI.

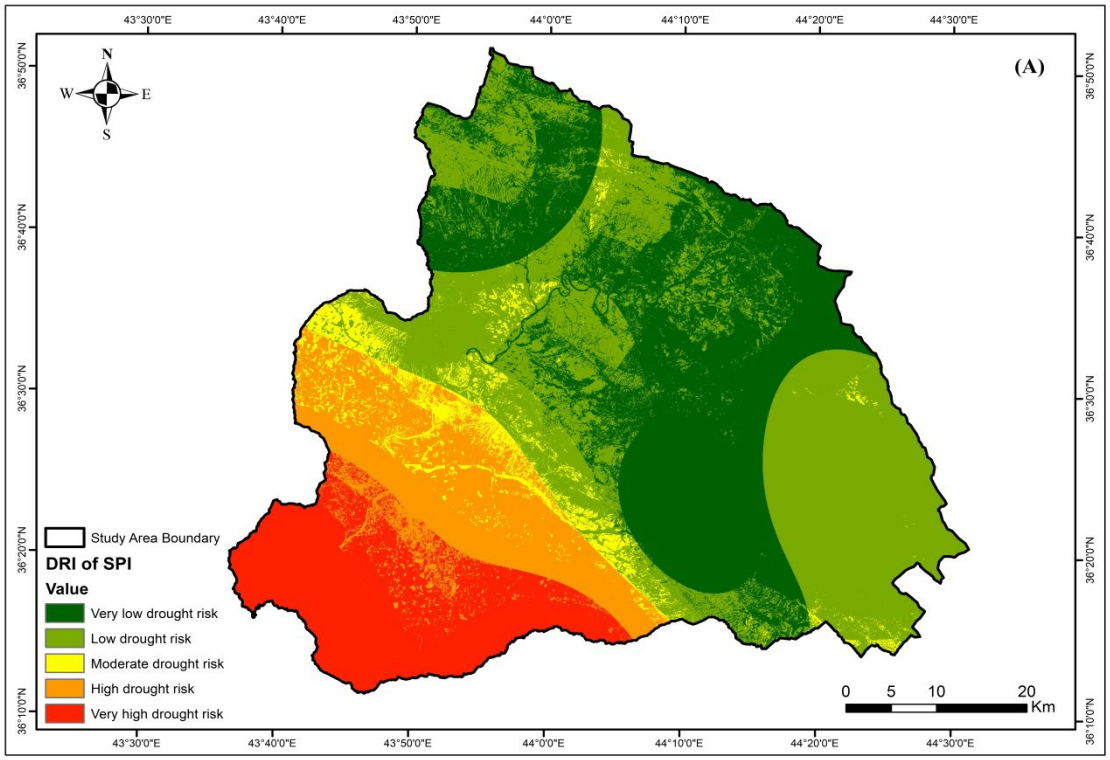

Figure 9: The DRI of the watershed based on SPI.

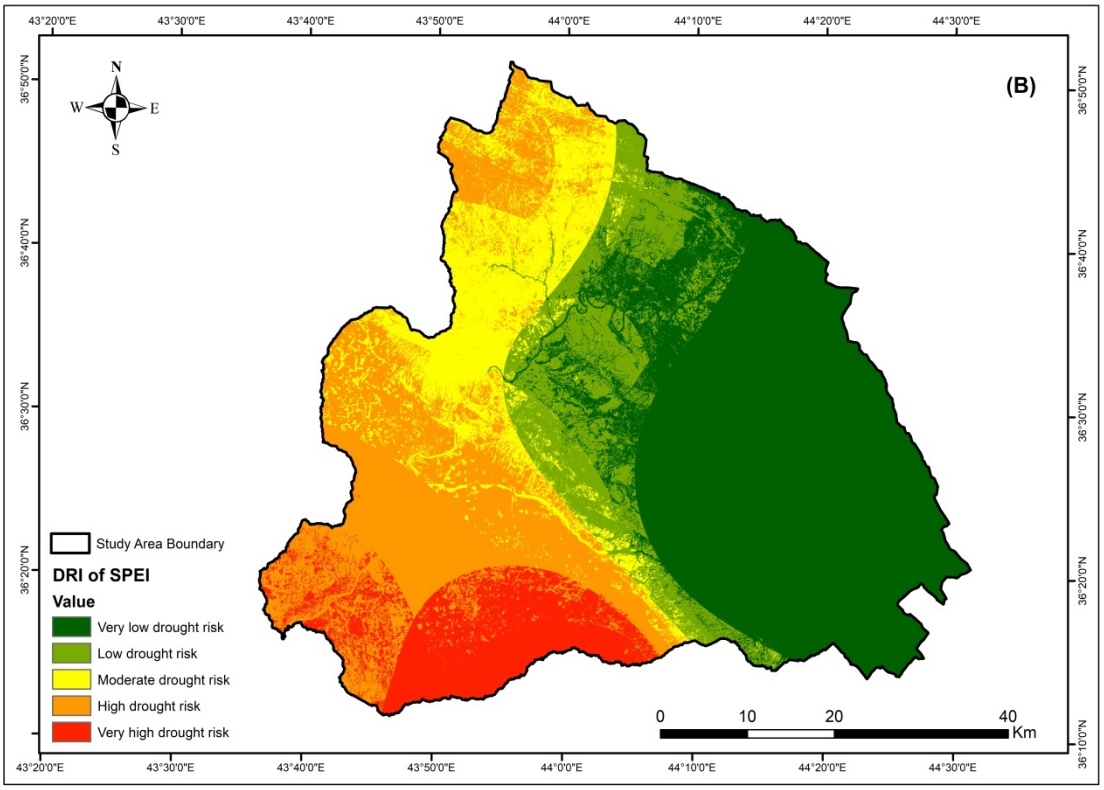

Figure 10: The DRI of the watershed based on SPEI.